Inversion of gravity anomaly due to a contact (fault) and its application for graben tectonics across Godavari basin

D. Ch. Venkata Raju, S. Ravikumar and D. C. Mishra*

National Geophysical Research Institute, Hyderabad 500 007, India

An inversion technique for gravity anomaly due to a contact (fault) using all the observation points along a profile is developed. Based on least-square inversion, the increments in different parameters are estimated and iterated to obtain the final model. Marquardt factor (λ) is used for quick convergence to the actual solution. This technique is tested on synthetic data for faults with different inclinations and with errors upto 20–30%. In most of the cases the computed values are within 5% of actual value. However, the computation is least sensitive to the inclination of the fault, and therefore its initial value is chosen very carefully to obtain a realistic model. A Bouguer anomaly profile across the Godavari basin, which shows a central 'low' corresponding to the Gondwana sediments and 'highs' along adjoining shoulders representing a typical graben structure, is chosen for application of the above technique. Removing a suitable regional, the Bouguer anomaly due to the central Gondwana basin is separated, and then fitted with the computed values using two different models: (i) a basin model of density contrast – 0.35 g/cc, and (ii) two contacts (faults) on either side of the basin with the same density contrasts. The characteristics of the contacts derived from the second model, including the maximum thickness of sediments, match quite well with those obtained from the first model and also with other known geological and geophysical information from the region. Both the contacts along the basin margin with adjoining basement rocks show deep inclination of 70–80 degrees, and the maximum thickness of sediments is approximately 5 km for a density contrast of – 0.35 g/cc. The nature of gravity anomaly along northern contact clearly indicates a faulted contact, while the southern side contact may be faulted only in specific sections.

As the contacts of rocks with different physical properties such as density or susceptibility indicate specific geological processes – faulting, folding, basin evolution, etc. – their mapping and quantitative evaluation are one of the most important aspects in geological sciences. Such contacts form good targets for gravity survey due to density contrast across them. Contacts, representing faults specially, provide typical antisymmetric gravity anomalies which can be easily identified and modeled to provide the characteristics of the faults. Several studies including inversion techniques, to model gravity anomalies due to faults have been reported[1]. However, a method in which the initial model can be chosen based on local geology and other available geophysical information, and where all the observation points can be used for inversion is preferred.

Before considering the inversion technique for gravity anomaly due to a contact fault, the theory behind it has been discussed. The expression for gravity anomaly $g(x)$ due to a contact of blocks with different densities at any point $P(x)$ along a profile perpendicular to the strike can be written as follows[1] (Figure 1):

$$g(x) = 2Gd[(x \sin Q - Z_1 \cos Q)(\sin Q \ln r_2/r_1 + \cos Q(\phi_2 - \phi_1) + Z_2\phi_2 - Z_1\phi_1)]. \quad (1)$$

Various symbols used in the equations (1) and (2) and explained in Figure 1, can be defined as: $g(x)$, gravity anomaly in mgals; G, universal gravitational constant; x, distance of the point of observation from the origin O; X, distance of the point of observation from the reference point R; D, distance of the origin from the reference point R; Z_1, depth to the top of the fault; Z_2, depth to the bottom of the fault; Q, dip of the fault plane (range is from 0 to 180°); d, density contrast between the two blocks on either side of contact which may represent a fault.

For a field profile, data can be obtained from a reference point. The origin is unknown. If D is the origin distance from the reference point R then equation (1) can be rewritten as:

$$g(x) = 2Gd[\{(X-D)\sin Q - Z_1 \cos Q\} + \{\sin Q \ln r_2/r_1 + \cos Q(\phi_2 - \phi_1)\} + Z_2\phi_2 - Z_1\phi_1], \quad (2)$$

where

$$r_1 = \sqrt{[(X-D)^2 + Z_1^2]},$$

$$r_2 = \sqrt{[\{(X-D) + (Z_2 - Z_1)\cot Q\}^2 + Z_2^2]},$$

$$\phi_1 = \pi/2 + \tan^{-1}(X-D)/Z_1, \text{ and}$$

$$\phi_2 = \pi/2 + \tan^{-1}\{(X-D) + (Z_2 - Z_1)\cot Q\}/Z_2.$$

This expression basically provides expression for the gravity anomaly due to a contact which may represent a fault. Interpretation of gravity profile implies solving the body parameters, viz. d, D, Z_1, Z_2 and Q. In our present study, the initial solution can be provided by known geology at the area or using any depth rules or characteristic curves. Then the computer calculates the theoretical anomaly using equation (2), and compares with the observed field. To compare the observed and

*For correspondence. (e-mail: postmast@csngri.ren.nic.in)

computed fields, one can define a objective function E as r.m.s. error between the two fields, which can be expressed as:

$$E = \sqrt{\sum_{i=1}^{N} (g_{\text{Obs}} - g_{\text{Cal}})^2 / N}\,, \tag{3}$$

where N = number of observations.

The r.m.s. error, E, should be minimum for a better match between the observed and the computed fields. However, in actual practice the interpreter must examine the computed models *vis-á-vis* known geology and other information from the region and judge judiciously which model fits best with them.

For optimization of the data, the procedure used is given below. The main aim is to minimize the r.m.s. error, E, between the observed and calculated anomalies. The error is reduced to a minimum if the initial solution is very close to the true solution. This can be obtained as:

If δd, δZ_1, δZ_2, δQ, and δD are the increments or decrements to be assigned to the parameters, the difference δg between the observed and calculated anomaly may be expressed as:

$$\delta g = \frac{\partial g(X)}{\partial d}\,\delta d + \frac{\partial g(X)}{\partial Z_1}\,\delta Z_1 + \frac{\partial g(X)}{\partial Z_2}\,\delta Z_2 + \frac{\partial g(X)}{\partial Q}\,\delta Q + \frac{\partial g(X)}{\partial D}\,\delta D\,. \tag{4}$$

Equation (4) can be expressed in matrix form for all the observations (N) as:

$$\bar{\mathbf{E}} = \bar{\mathbf{A}}\,\bar{\mathbf{P}}, \tag{5}$$

where, $\bar{\mathbf{E}}$ is the error matrix of order $N \times 1$ obtained by subtracting the calculated anomaly from the observed anomaly, $\bar{\mathbf{A}}$ is the matrix of order $N \times 5$ (Jacobian matrix) obtained by taking the partial derivatives w.r.t. parameters, and $\bar{\mathbf{P}}$ is the matrix of order 5×1 which contains increments or decrements of the parameters.

The parameter matrix $\bar{\mathbf{P}}$ can be obtained by the following equation:

$$\bar{\mathbf{P}} = \mathbf{A}^{-1}\bar{\mathbf{E}}. \tag{6}$$

$\bar{\mathbf{A}}$ may not be a square matrix and therefore its transpose, $\mathbf{A}^{\mathrm{T}}$, is used to get the parameter matrix[2].

$$\bar{\mathbf{P}} = [\mathbf{A}^{\mathrm{T}}\bar{\mathbf{A}}]^{-1}\,\mathbf{A}^{\mathrm{T}}\,\bar{\mathbf{E}}. \tag{7}$$

Most of our geophysical problems are over determined, i.e. the number of observations are more than the number of unknown parameters (body parameters). So equation (7) gives a least square solution to the parameter matrix. However, if initial solution is not close to the actual solution, convergence becomes difficult. To overcome this problem, Marquardt factor λ is used and equation (7) becomes[3]:

$$\bar{\mathbf{P}} = [\mathbf{A}^{\mathrm{T}}\bar{\mathbf{A}} + \lambda\bar{\mathbf{I}}]^{-1}\,\mathbf{A}^{\mathrm{T}}\bar{\mathbf{E}}. \tag{8}$$

In equation (8), $\bar{\mathbf{I}}$ is an identity matrix, $\mathbf{A}^{\mathrm{T}}$ is the transpose of $\bar{\mathbf{A}}$, and λ is the Marquardt damping factor. When $\lambda = 0$, the algorithm is equal to Newton's Gauss method. This method is good for good initial solution. If the initial solution is far from the true solution then it leads to a divergent solution. If λ is very large then this algorithm is close to steepest descent method. It takes a long time but converges for poor initial solution also. In this method, we assign $\lambda = 1$ or 0.1 as the initial value. By dividing the value by three each time λ is successively reduced, if the objective function is less than the existing value, otherwise it is multiplied by a factor 2, the modified parameters can be obtained as follows:

$$d = d + \delta d, \quad Z_1 = Z_1 + \delta Z_1, \quad Z_2 = Z_2 + \delta Z_2$$

$$Q = Q + \delta Q, \quad D = D + \delta D. \tag{9}$$

By using the modified parameters given by equation (9), theoretical anomaly is again calculated, using equation (2). The parameters may be further modified in an iterative way till the error, E, is minimum. The program is terminated either after the specified numbers of iterations are completed or when the Marquardt parameter assumes a very large value or the r.m.s. error is reduced to a minimum value.

In practice, gravity anomaly along a profile perpendicular to strike direction can be digitized at suitable station interval from a reference point (from one end). The distance vs gravity field (Bouguer anomaly) is given to the computer as input data. The initial parameters of the model and Marquardt parameter ($\lambda = 0.1$ or 1.0) are also given as input to the computer. Computer modifies the solution in an iterative way till one of the conditions specified above is satisfied. The final parameters and the corresponding computed field are obtained as the output.

Theoretically-computed gravity anomaly with following parameters: $Z_1 = 1.0$, $Z_2 = 20.0$, $D = 121.0$, $d = 0.35$, and $Q = 90°$ was generated and plotted in Figure 1. The distance vs computed field along with initial solution are given as input to the computer for inversion. The program is tested on the above data by giving initial solution with 20–30% error in the parameters. The observed and fitted data with final parameters are given in Figure 1, which is almost within 5% of the actual solution. Figure 2 shows gravity anomaly for $Q = 30°$

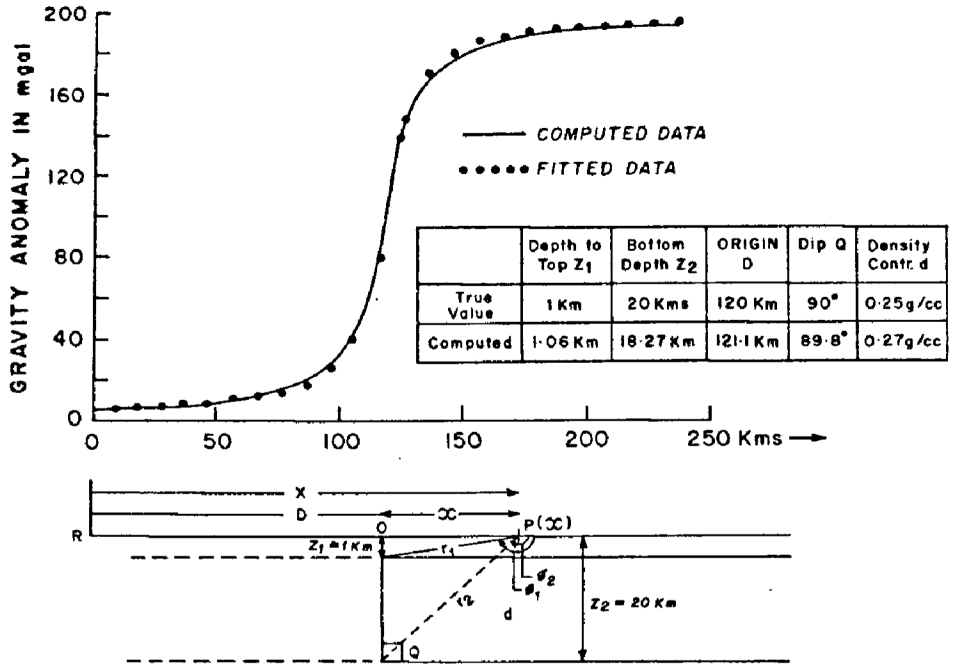

	Depth to Top Z_1	Bottom Depth Z_2	ORIGIN D	Dip Q	Density Contr. d
True Value	1 Km	20 Kms	120 Km	90°	0·25g/cc
Computed	1·06 Km	18·27 Km	121·1 Km	89·8°	0·27g/cc

Figure 1. Contact (Fault) model for $Q = 90°$, and corresponding theoretically computed gravity field. The parameter of the model and computed parameters obtained from the inversion of the field are given in the inset of the diagram for a comparison. The initial value for inversion is provided with 30% error.

and 60° inclinations of contact (fault). It may be noticed that for different inclinations (Q) of fault, there is very small shift in the computed profiles and therefore one has to be very cautious in providing initial value of Q. The approximate value of Q and D may be chosen based on the local geology or other geological information from the region.

Discussed in this section is a field example. Fault models are most important for rift basins which are controlled by normal faults on either margins. The most important rift basin in this country is Godavari basin which extends almost from east coast of India near Masulipatnam upto central India, south of Chandrapur, striking NW–SE (Figure 3). It is occupied by Gondwana sediments represented by sandstones, shales, limestones, etc. of Permian–Jurassic period[4]. The Bouguer anomaly map (Figure 3), Mishra *et al.*[5], shows a linear gravity 'low' over the sediments, and gravity 'highs' along the shoulders, which are typical of rift valleys. The sharp gravity gradient towards north indicates the master fault of the basin, while towards south it appears to have faulted contact in sections where gradient is sharper compared to other places. A profile AA′ across the basin is reproduced in Figure 4, which shows central 'low' with adjoining 'highs' on either side. In a gravity model Mishra *et al.*[6] inferred the central 'low' due to 5–6 km thick Gondwana sediments of density contrast −0.35 g/cc, and the adjoining 'highs' due to the high density material in the crust along the shoulders.

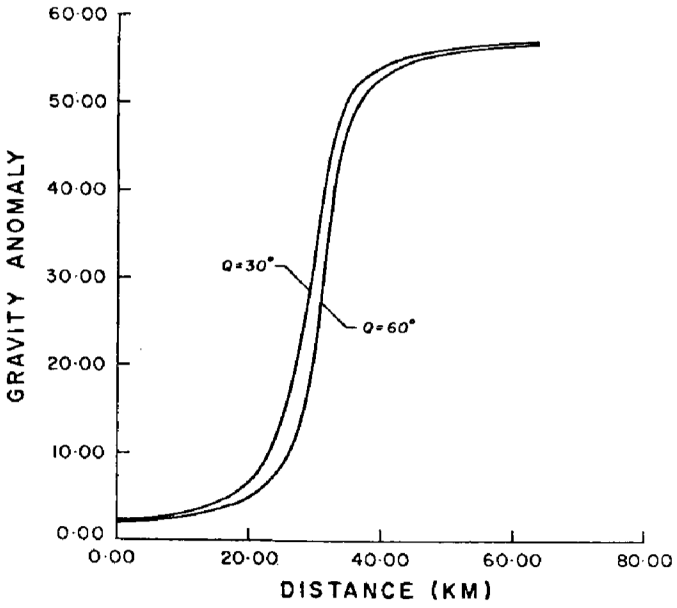

Figure 2. Computed field for $Q = 30°$and 60° with $Z_1 = 1$ km and $Z_2 = 5$ km for a density contrast of 0.35 g/cc. It shows almost similar anomaly for both inclinations of the contact plane only with a little shift.

Examining the Bouguer anomaly map, it is noticed that the contour of −40 mgal coincides almost with the southern margin of the basin and deflects outside the basin. Similarly, towards the northern margin, the −35 mgal contour deflects outside the basin, and encloses

the adjoining high. Therefore, taking a -40 mgal level towards the southern flank and -35 mgal level towards the northern flank, a regional level to separate the gravity anomaly due to Gondwana sediments is drawn (Figure 4). It is apparent from the Bouguer anomaly along this profile that regional field has a gradient towards south. Subtracting the observed Bouguer 'low' from this regional level, the anomaly BC due to low density sediments of Gondwana basin is obtained (Figure 5). This residual field can be modeled in two ways: (i) using a basin model[7], and (ii) using contact models on either flanks as described above. The residual anomaly BC can be considered to be composed of two parts BB′ and CC′ (Figure 4), which are similar to the gravity anomaly due to a contact (fault), and corresponds to the contacts on either flank of the rift basin.

Using the basin model the Bouguer anomaly at equidistant interval with respect to initial point is provided as input to the computer programme which computes the thickness of sediments using the expression for a slab[7] and provides the depths to the basement at these points. The results of modelling of the profile BC for a density contrast of -0.35 g/cc is shown in Figure 5, which indicates that the maximum thickness of sediments is about 5.1 km. It also shows the northern margin as a simple fault. Mishra *et al.*[5], termed it as the master fault of the rift basin. The southern flank shows faulting in specific sections, specially towards the bottom part of the basin.

Using the contact (fault) model the components of Bouguer anomaly BB′ and CC′ are modeled with similar density contrast of -0.35 g/cc. The initial value for

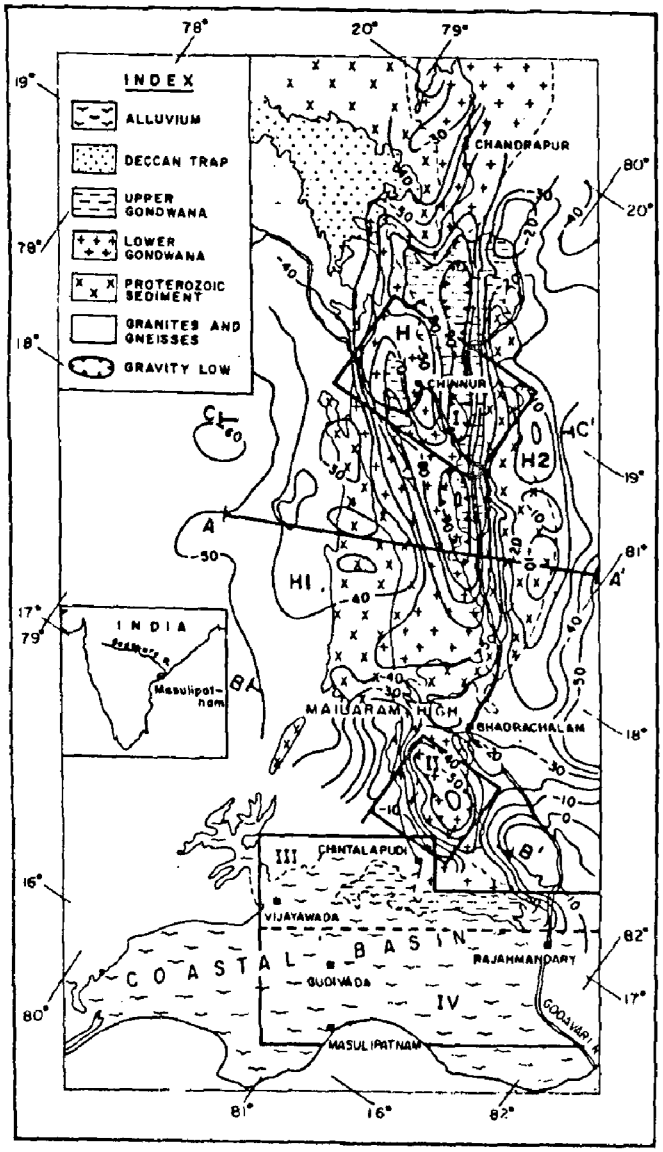

Figure 3. Bouguer anomaly map of Godavari basin with superimposed geology. It shows a linear gravity 'low' over Gondwana sediments and 'high' along adjoining shoulders. The northern contact of the basin shows a sharp gradient indicating master fault of the rift basin.

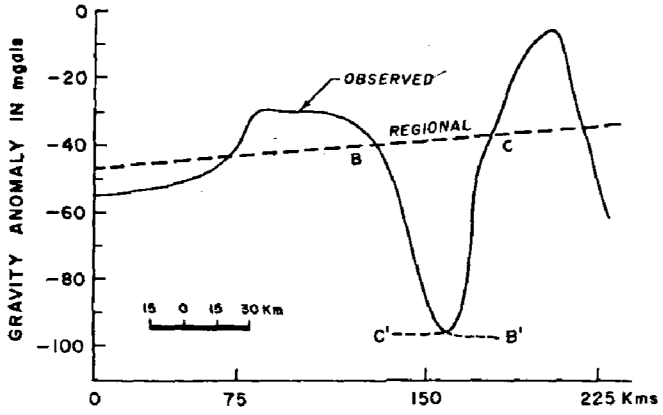

Figure 4. Profile AA′ across Godavari basin taken from Bouguer anomaly map (Figure 3). It shows observed Bouguer anomaly and the regional field based on the values of Bouguer anomaly along either contacts of Gondwana sediments.

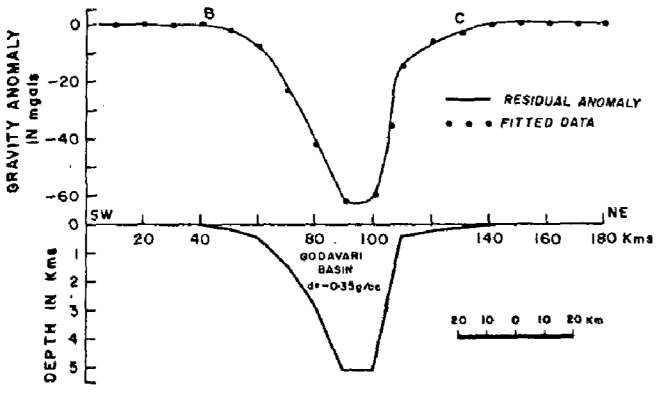

Figure 5. Residual Bouguer anomaly due to Gondwana sediments obtained by subtracting regional field from the observed field in the central part of profile AA′ (Figure 4). The basin model obtained from the inversion of residual anomaly is shown at the bottom of this figure. *d* is the density contrast between Gondwana sediments and the adjoining basement.

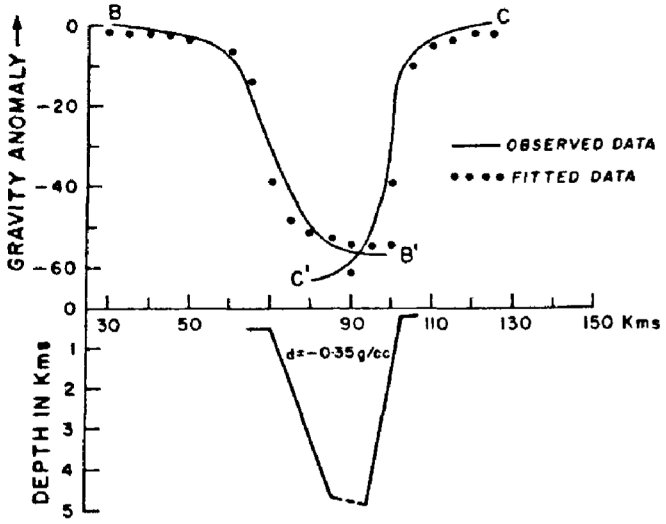

Figure 6. Contact (Fault) model obtained from the inversion of either flanks of residual anomaly given in Figure 5.

origin distance D is provided based on exposed Gondwana sediments along the profile. The results are presented in Figure 6, which shows the maximum thickness of sediments as 4.9 km towards the northern flank and the maximum thickness of sediments along the southern flank as 4.6 km. The r.m.s. errors for gravity anomaly BB′ and CC′ (Figure 6) are 0.102 and 0.072 respectively. The difference between the computed thickness of sediments along the two sides can be attributed to the difference in the elevation on either side of the Godavari basin, which is 400–500 m higher towards the northern flank. Both the northern and southern flanks are shown as faults, though the northern side fault is more steeper (80°) than the southern side (70°).

DSS profile across Chintalpudi sub-basin (Kaila *et al.*[8]), has provided a thickness of 2.8 km of lower Gondwana sediments in this region. Therefore in Godavari sub-basin where both lower and upper Gondwana sediments are deposited, the total thickness of Gondwana sediments is expected to be more than this value. Raju[9] (1986) reported 4.5 km thickness of sediments based on geological and geophysical studies in this region.

Mishra *et al.*[5], have used the method of direct computations of gravity field due to multiple bodies and compared it with the observed field. In this approach there is a considerable amount of bias due to interpreter which will provide a biased solution. However, the present method is based on the inversion of the observed gravity field and therefore there is no bias in it. The maximum thickness of sediments derived from the two models are compatible. The thickness of sediments estimated by Mishra *et al.*[5], based on computation of gravity field due to multiple bodies including high density bodies along the shoulders of the graben, is in agreement with the present study. This confirms the appropriateness of the model used and the inversion technique employed in our work.

1. Radhakrishna Murthy, I. V. and Mishra, D. C., AEG publication, 1989, pp. 1–300.
2. Jackson, D. D., *Geop. J. R. A. Soc.*, 1972, **28**, 97–108.
3. Marquardt, D. W., *J. Soc. Indian Appl. Math.*, 1963, **11**, 431–441.
4. Fox, C. S., *Mem. Geol. Surv. India*, 1931, 58.
5. Mishra, D. C., Gupta, S. B., Rao, M. B. S. V., Venkatrayudu, M. and Laxman, G., *J. Geol. Soc. India*, 1987, **30**, 469–476.
6. Mishra, D. C., Gupta, S. B. and Venkatrayudu, M., *Earth Planet. Sci. Lett.*, 1989, **94**, 344–352.
7. Radhakrishna Murthy, I. V. and Krishnamacharyulu, S. K. G., *Computers Geosci.*, 1990, **16**, 539–548.
8. Kaila, K. L., Murthy, P. R. K., Rao, V. K. and Venkateswarlu, N., *Tectonophysics*, 1990, **173**, 307–317.
9. Raju, P. S. R., *J. Assoc. Explo. Geophys.*, 1986, **7**, 131–146.

ACKNOWLEDGEMENTS. We thank Prof. I. V. Radhakrishna Murthy for his discussions with S.R. and providing him with his basin model programme.

Received 25 March 1998; revised accepted 29 September 1998

Pattern of growth and utilization of abdominal fat bodies during larval development and metamorphosis in five South Indian anurans

N. P. Gramapurohit, B. A. Shanbhag* and S. K. Saidapur

Department of Zoology, Karnatak University, Dharwad 580 003, India

The tadpoles of *Rana tigrina, Rana cyanophlyctis, Rana curtipes, Polypedatus maculatus* and *Bufo melanostictus* grew in size (mass and snout vent length or SVL) progressively until metamorphic climax. The abdominal fat bodies first appeared in stages 25–30; and accumulation/utilization of fat during larval development and metamorphosis varied with the species. In *B. melanostictus*, fat bodies were barely seen. In laboratory-reared *R. curtipes*, body weight and fat body mass were better developed than in the wild caught. The amount of fat deposition was related to the duration of metamorphosis in the various species studied. The findings thus show that the size of fat bodies in the larval anurans is correlated with the body mass, SVL as well as duration of metamorphosis.

THE conspicuous nature of abdominal fat bodies and seasonal and/or annual changes in their mass in adult anurans are well documented[1–3]. Such changes in the fat body mass in amphibians indicate changes in the nutritional status of a given individual[4]. The abdominal

*For correspondence.